

Methodology of electron Bernstein wave emission simulations

J. Urban¹, J. Preinhaelter¹, V. Shevchenko², G. Taylor³, M. Valovic²,

P. Pavlo¹, L. Vahala⁴, G. Vahala⁵

¹ EURATOM/IPP.CR Association, Institute of Plasma Physics, 182 21 Prague, Czech Rep.

² EURATOM/UKAEA Fusion Association, Culham Science Centre, Abingdon, UK

³ Princeton Plasma Physics Laboratory, Princeton, New Jersey 08543, USA

⁴ Old Dominion University, Norfolk, VA 23529, USA

⁵ College of William & Mary, Williamsburg, VA 23185, USA

Abstract. Electron Bernstein wave (EBW) emission, via mode conversion to ordinary and extraordinary waves, is typical for devices with high-density plasmas and low magnetic field, such as spherical tokamaks (ST) and stellarators. Our studies are primarily focused on EBW emission from spherical tokamaks. To interpret experimental EBW experimental data we use a 3D numerical simulation code, which consists of an antenna model, an EBW-X-O conversion efficiency computation and ray tracing. We present simulation results for the MAST and NSTX STs. Possible utilizations of EBW emission, e.g. electron temperature measurement or magnetic field reconstruction, are discussed.

Electron Bernstein waves. Electron Bernstein waves (EBW) are electrostatic waves, which propagate in hot magnetized plasmas only. They are not subject to density limits like electromagnetic ordinary (O) and extraordinary (X) waves and they are the only modes in electron cyclotron frequency range that can propagate in overdense (high β) plasmas in spherical tokamaks or stellarators. EBW are not usually detected (launched) directly, but rather O and X modes, originating at the upper hybrid resonance (UHR) layer by EBW-X and EBW-X-O mode conversion processes, are detected by antennas out of the plasma [1].

Antenna and plasma models. For the present MAST EBW radiometer [2, 3], the Gaussian beam formalism is used to find the positions of the first waist at the horn mouth and the second waist beyond the lens. Polarization changes by the reflection at the mirrors are taken into account. The radiometer can detect linearly polarized waves only, within the frequency range 15 – 60 GHz by fast sweeping of the detected frequency. Calibration is performed on shot-to-shot basis by measuring the radiation of an empty torus. For the NSTX EBW radiometer, the Gaussian beams are used as well, but the beam is numerically simulated until the last waist. The NSTX radiometer [4] presently detects 16-18 GHz plasma emission in two perpendicular linear polarizations and is absolutely calibrated.

In our simulations, mostly the EFIT equilibrium reconstruction code is used. In particular, we read $\psi(R,Z)$ and $F(\psi)$ data and interpolate them using high order B-splines. Assuming toroidal symmetry, this provides a 3D magnetic configuration of the plasma. The electron temperature and density profiles are obtained from Thomson scattering measurements,

which provide radial profiles of these quantities. By splining of the temperature and density data and mapping to magnetic flux surfaces, we construct a 3D model of the plasma.

Simulation code. The numerical simulation starts at the plasma boundary. At the last waist before the plasma, we construct a 41-ray model of the beam – 5 circles of 8 rays plus 1 central ray. The rays are projected (the beam divergence is taken into account) onto the plasma last close flux surface (LCFS) to define the spots where we start the numerical simulation. Since the EBW emission and mode conversion is reciprocal, the waves are simulated as they propagate from the antenna into the plasma.

At the intersection of the antenna pattern and the LCFS, an auxiliary plane stratified plasma slab is constructed along the density gradient. The slab model is used for the conversion efficiency computation and for solving the hot dispersion relation to obtain initial conditions for the ray tracing.

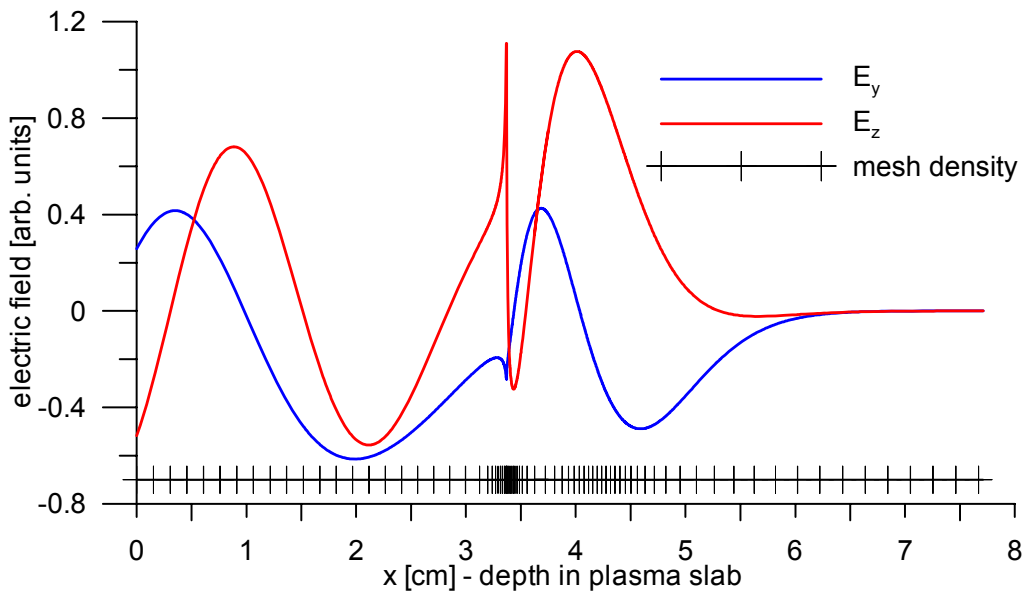


Fig. 1: Full wave solution in cold plasma slab. NSTX shot #113544, $t=0.325$ s, $f=16.5$ GHz. x axis parallel with the density gradient, z axis parallel with the magnetic field.

To obtain the EBW-X(-O) conversion efficiency, we solve Maxwell equations in the cold plasma slab. With inhomogeneity in one direction only, this involves solution of two second order ordinary differential equations (ODE) with boundary conditions. Because of the cold plasma, we have to introduce small artificial collisions to avoid the singularity at the UHR. Then, the power absorbed by the collisions at the UHR equals the power in the EBW. To solve the ODE's we have developed a finite elements code with adaptive mesh refinement [5], designed specially for boundary value problems and strong diversity of mesh density requirements along the computational domain (Fig. 1). Close to the UHR and plasma resonance regions, the solution is almost singular and requires a much denser mesh. The ray-tracing code uses 4th order Runge-Kutta method to solve the ray equations, which describe the EBW packet motion. The power evolution equation $dP/d\tau = -2\gamma(\tau)P$ and the

radiative transfer equation $dP/d\tau = \eta - \alpha P$ must be solved along the ray [6]. The emitted power can be expressed by the Rayleigh-Jeans formula with radiative temperature T_{rad} : $P \sim \omega^2 T_{rad}$. Both collisional and non-collisional damping (emission) are considered.

The final simulated intensity is then

$$I_{ECE} = const \times \iint dS W_{Gauss} C_{EBW-X-O} \omega^2 T_{rad} C_{window} V_{relat}, \quad (1)$$

where $C_{EBW-X-O}$ is the conversion efficiency, $\omega^2 T_{rad}$ is the Rayleigh-Jeans formula, C_{window} is the power transmission coefficient of the vacuum window, V_{relat} is the relative visible area and W_{Gauss} is the Gaussian weight. The integration is over the intersection of the beam waist and the projection of the vacuum window to the waist plane, after interpolating all the values across this area.

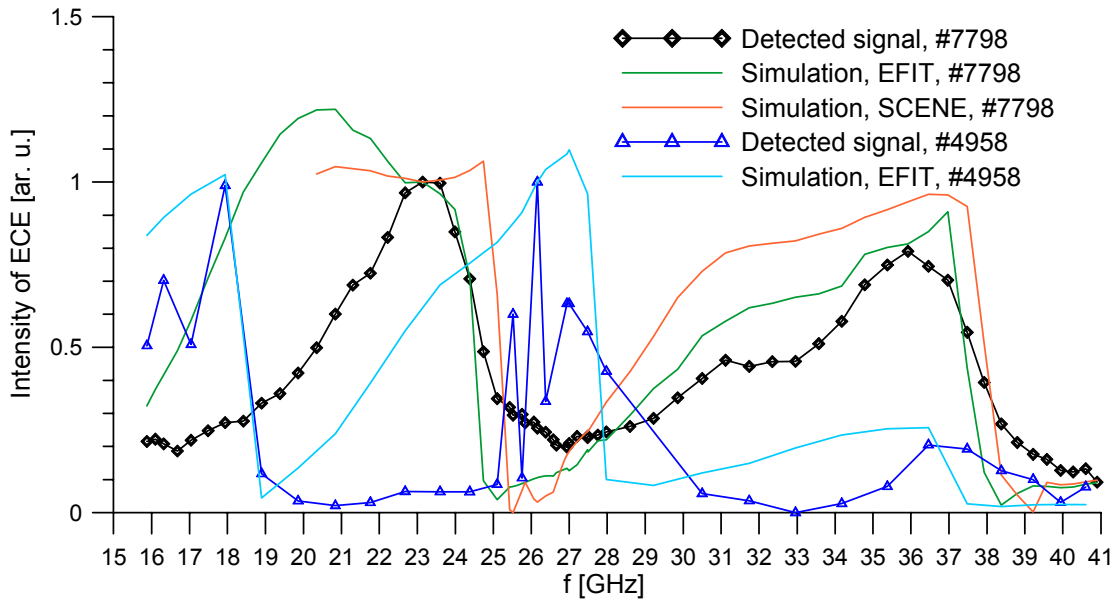


Fig. 2: Comparison of detected and simulated ECE signals, MAST, shots #7798 ($t=280$ ms) and #4958 ($t=120$ ms).

Results. For the MAST tokamak, we have achieved good results for simulating the whole EBW emission spectra for one particular time per shot (the time of the high spatial Thomson scattering measurements), see Fig. 2. Recent results for some H-modes indicate that the magnetic field at the plasma edge is greater than the EFIT equilibrium field. Thus, we have created a model, which estimates a magnetic field correction so the EBW emission simulation agrees better with the experimental data (Fig. 3). The simulated time development of central electron temperature in NSTX tokamak fits well the measured signal (Fig.4) and proves that the EBW emission measurement can be used as an electron temperature diagnostics on NSTX. Recently we modified our code for 3D configurations, primary for WEGA stellarator simulations, and these results will be presented elsewhere.

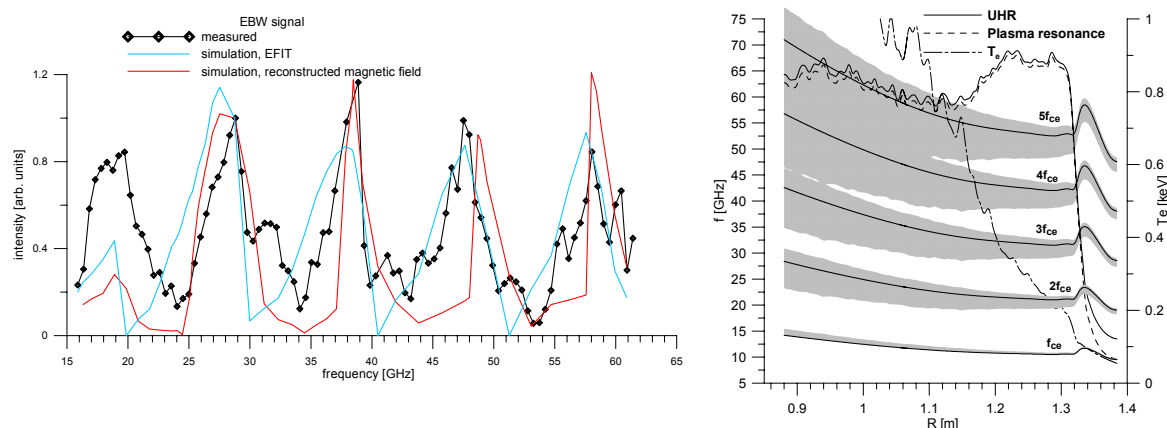


Fig. 3: MAST shot #8694, t=280 ms. Comparison of two simulations (EFIT and reconstructed magnetic field) with experiment (left), reconstructed magnetic field (right).

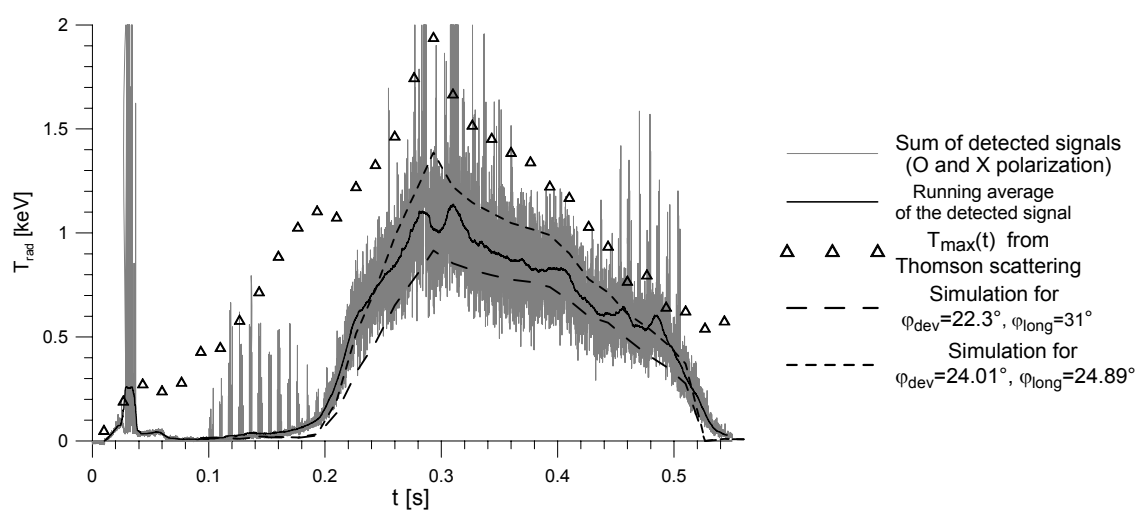


Fig. 4: The time development of EBW signal detected by the NSTX antenna operating at 16.5GHz. Shot #113544.

Acknowledgements. Supported by U.S. Dept. of Energy, by UK Engineering and Physical Sciences Research Council, by EURATOM and by AS CR project #AV0Z-20430508.

References

- [1] V. Kopecky, J. Preinhaelter: *Linear Mode Conversion in Inhomogeneous Magnetized Plasma*, Academia Praha (1983).
- [2] J. Preinhaelter, V. Shevchenko, M. Valovic, et al., ECA Vol. **28G**, P-4.184 (2004).
- [3] J. Preinhaelter, J. Urban, P. Pavlo, et al., Review of Scientific. Instruments **75**, p. 3804 (2004).
- [4] G. Taylor, P.C. Efthimion, B.P. LeBlanc, et al., Phys. Plasma **12**, pp. 052511 1-7 (2005).
- [5] J. Urban, J. Preinhaelter, Czech. J. Phys. **54**, Suppl. C, C109-C115 (2004).
- [6] M. Bornatici et al, Nucl. Fusion **23**, 1153-1257 (1983).